Advanced Ceramics Progress: Vol. 8, No. 1, (Winter 2022) 36-43

Materials and Energy Research Center
MERC

Contents lists available at ACERP

Advanced Ceramics Progress

Journal Homepage: www.acerp.ir

Original Research Article

Effect of Temperature on the Low-Pressure Chemical Vapor Deposition of Graphene

Aziz Noori [a], Mohammad Javad Eshraghi [b], Asieh Sadat Kazemi [c, *]

[a] *MSc Student, Department of Physics, Iran University of Science and Technology (IUST), Tehran, Tehran, Iran*
[b] *Associate Professor, Department of Semiconductors, Materials and Energy Research Center (MERC), Meshkindasht, Alborz, Iran*
[c] *Assistant Professor, Department of Physics, Iran University of Science and Technology (IUST), Tehran, Tehran, Iran*

* Corresponding Author Email: asiehsadat_kazemi@iust.ac.ir (A. S. Kazemi)

URL: https://www.acerp.ir/article_153519.html

ARTICLE INFO

Article History:

Received 30 May 2022
Received in revised form 28 June 2022
Accepted 17 July 2022

Keywords:

Graphene
Chemical Vapor Deposition
Growth Temperature
Raman Spectroscopy
Atomic Force Microscopy

ABSTRACT

Large area fabrication of graphene, as a leading two-dimensional material as well as an allotrope of carbon, is a challenging requirement prior to its preparation for applications. Chemical Vapor Deposition (CVD) is one of the most effective and promising methods for high-scale and high-quality synthesis of graphene. In this study, graphene layers were grown on copper (Cu) sheets using low-pressure CVD technique at 930 °C, 870 °C, and 760 °C. Raman spectroscopy, Field Emission Scanning Electron Microscopy (FESEM), Optical Microscopy (OM) and Atomic Force Microscopy (AFM) were employed in this study to investigate the effect of the process temperature on the structural properties, morphology, grain boundaries, continuity, purity, and number of layers. The results from analyses revealed that at higher temperatures, the continuity and quality of the layers and number of grain boundaries were higher and lower, respectively. In contrast, at lower temperatures, the nucleation and discontinuity of the deposited layers were relatively high. The surface roughness of the graphene sheets increased with a decrease in temperature.

https://doi.org/10.30501/acp.2022.343786.1090

1. INTRODUCTION

Two-Dimensional (2D) materials have attracted considerable attention due to their properties that are superior to those of their 3D counterparts. These materials are regarded as the potential candidates for replacement of conventional resources in many fields of technology. Further, they have introduced new applications in some areas, but a complete replacement of these materials faces several challenges such as ensuring the mass production, high purity, and efficient utilization [1,2].

A leading member of the 2D family [2,3], graphene, is a unique material due to its excellent properties such as high electrical and thermal conductivity [5], high density [6], high optical conductivity [7], and excellent mechanical properties [8,9]. A layer of carbon atoms in graphene is packed in a honeycomb network with sp^2 hybridized orbitals and a bond length of 0.142 nm [8,9].

Please cite this article as: Noori, A., Eshraghi, M. J., Kazemi, A., "Effect of Temperature on the Low-Pressure Chemical Vapor Deposition of Graphene", ***Advanced Ceramics Progress***, Vol. 8, No. 1, (2022), 36-45. https://doi.org/10.30501/acp.2022.343786.1090

Graphene can be fabricated using different methods such as mechanical exfoliation [11], electrochemical exfoliation [12], liquid-phase exfoliation [13], peer growth on silicon carbide (SiC) [14], unzipping of carbon nanotubes [15], and graphene oxide reduction [16]. Exfoliation methods used for graphene production produce very small flakes with random thickness values while reduction methods would form several layers. These are not continuous and still have residues left behind from the synthesis method. However, large area graphene with controlled number of layers can be obtained by Chemical Vapor Deposition (CVD) [17]. In CVD, the required carbon atoms are separated from the precursor gas under high temperature and low pressure and then bonded with a flat metal sheet [18]. CVD is an extensive bottom-up method for synthesizing multilayer and monolayer graphene films. This approach outperforms other methods in terms of its ease of installation in laboratories, successful long-term use in industrial environments, high potential for large-scale production, and beneficial environmental and economic factors [19]. The process and types of different chemical reactions that occur in a CVD chamber are controlled by many complex factors including system regulation, furnace configuration, gas bare materials, gas ratios, chamber pressure, gas flow, reaction temperature, and growth time [20,21].

There are several types of CVD methods available today that can be used to synthesize graphene-based materials. Following its first isolation via micromechanical exfoliation in 2004, larger area graphene was successfully obtained using Low-Pressure CVD (LPCVD) [22]. Historically, CVD growth of the crystalline graphite on Ni was first reported in 1966 [23] and later, graphite was deposited on Pt using CVD [24]. Ever since, LPCVD has been used to grow graphene with the advantage of obtaining more uniform sheets with few layers [25].

Depending on the growth conditions, different CVD methods can be classified into several main types based on temperature, pressure, precursor nature, gas flow, wall/bed temperature, deposition time, and activation energy [26,27]. Among the mentioned factors, temperature plays a vital role in CVD growth of graphene since it provides the required activation energy to decompose the carbon source and prepare the substrate surface. For instance, the required temperature for methane decomposition is about 1000 °C [28]; therefore, graphene cannot be formed below this temperature. However, graphene can be synthesized at lower temperatures using other materials in the growth process [29-31]. Under the same laboratory conditions, temperature variations cause changes in the growth quality, number of layers, and continuity of the grown layers. Chaitoglou et al. [32] explored the effect of temperature on the CVD graphene growth on Cu. In their research, the temperature varied from 970 °C to 1070 °C, and no roughness study was conducted. In another study, the optical transmittance spectra were used to determine the number of the graphene layers grown at 400-1000 °C via CVD. Lower temperatures resulted in lower quality graphene films [33]. Zheng et al. [34] reported catalytic metal engineering to reduce the growth temperature to 700 °C using Cu-C alloy on SiO_2/Si substrate and CVD growth of continuous single-layer graphene on Cu by sequential melting-resolidification-recrystallization in the temperature range of 980-1060 °C. The latter required a complicated and costly process, yielding the results comparable to those of the usual CVD methods.

Here, graphene was grown by LPCVD method in a homemade LPCVD setup at temperatures around and well below the usual temperature (1000 °C) required for decomposition of the carbon precursor. Cu substrate was used as the catalyst and methane (CH_4), as a carbon precursor. The dependency of temperature on the growth quality, continuity, and number of graphene layers was investigated at 930, 870, and 760 °C using different surface analysis methods. While Raman spectra and FESEM results confirmed the formation of graphene sheets, surface roughness parameters obtained from atomic force microscopy images yielded novel results regarding the as-grown graphene sheets on Cu. Many large area graphene sheets are characterized by high roughness values that limit their applications, hence roughness control based on growth parameters is very beneficial.

2. MATERIALS AND METHODS

In this study, 99.99 % H_2 and 99.9 % CH_4 were used as the assistant and carbon source gases, respectively, due to the following reasons: a) hydrogen is widely used in the annealing phases to remove the oxide layer on the metal surfaces, and b) it plays a key role in absorbing H_2 from CH_4 [17]. Methane has a single bond and lower bond energy than a carbon precursor with a double and triple bond whereas acetylene with its triple bond character can react with unbonded electrons of other elements in the environment. Therefore, unwanted corrosive and toxic compounds may be produced from these reactions [35]. In this study, Cu foils with a thickness of 30 µm were used as the substrate, and the thermal decomposition of methane was reduced by 930, 870, and 760 °C to control the growth procedure in the presence of Cu as the catalyst substrate. Here, Cu was selected for the growth process due to the lower solubility of C atoms in Cu. It is known that C solubility in Ni is higher. Furthermore, thin film Cu catalyst sheets are readily available and inexpensive [36].

The foils were cut into sheets of 20×50 mm^2 in size. Cu sheets were initially immersed in acetic acid (99.9 %, Merck) for 10 min to remove surface oxides and then washed in ethanol for five min in an ultrasonic bath to

remove impurities and contaminations. Cu sheets were then air-dried for two minutes. Finally, they were transferred via an alumina boat into a quartz chamber in the furnace.

Figure 1 shows the schematics of the home-made LPCVD system which is used for growing graphene on the Cu sheets. As indicated in this figure, this setup consists of a tubular furnace, Mass Flow Controllers (MFC) for controlling gas flows, a vacuum gauge for controlling the deposition pressure, and a rotary vacuum pump with a volume capacity of 80 m^3/h for evacuating the by-products.

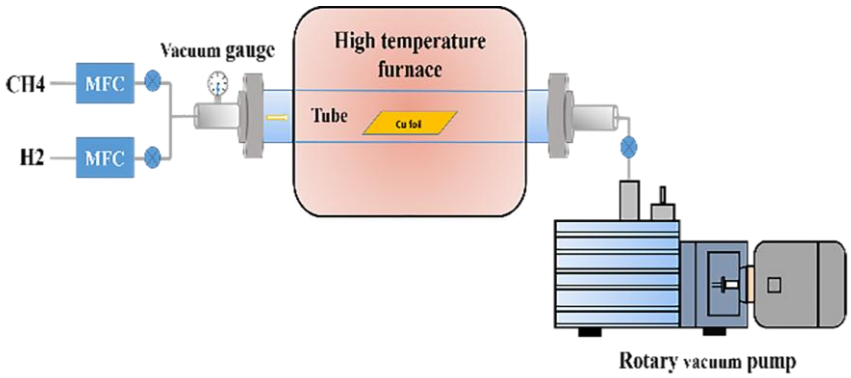

Figure 1. Schematics of the LPCVD setup for graphene growth

CH_4 and H_2 flow rates were set at 35 and 7 (standard cubic centimeter/minute) sccm, respectively, to maintain the flow ratio of 5:1. The initial pressure of the chamber was set at 0.35 mbar. At 200 °C, H_2 was allowed into the furnace to prevent Cu oxidation. CH_4 entered the chamber at the desired coating temperature. At the end of deposition, CH_4 flow was stopped, and the furnace cool-down stage was performed in the H_2 atmosphere. Finally, the samples were extracted from the furnace at the ambient temperature. Of note, the samples grown at 930, 870, and 760 °C are named S1-S3, respectively, hereafter. In addition to the fabrication of Samples S1-S3 at different temperatures, and for a comparative study, a Cu sheet was annealed at 930 °C in the presence of H_2 and in the absence of CH_4. This sample is called bare-Cu hereafter. The time required for the growth process for all samples was fixed at 30 min. The specific values of the growth temperatures were obtained from experimental trials.

Optical microscopy (Nano Raga), Field Emission Scanning Electron Microscopy (FESEM-TESCAN Mira3 operated at 15 kV), and Atomic Force Microscopy (AFM-Advanced Ara Pajauhesh) were used to characterize the structural and surface properties of the obtained graphene sheets. Raman spectroscopy (Teksan 530-700 nm wavelength) was also used to ensure the formation of graphene.

3. RESULTS AND DISCUSSION

Carbon atoms settle together on a Cu sheet during the CVD growth of graphene, as indicated in Figure 2.

During the growth mechanism, Cu, as the metal catalyst, determined graphene's precipitation rate and was exploited to reduce the energy barrier of the reactions. It should be noted that C atoms are slowly adsorbed on the Cu surface. With CH_4 entrance in the furnace and the increase of the temperature to values required for the decomposition of hydrocarbon bonds, and C atoms precipitate as a solid on the Cu surface while H atoms bond together and leave the chamber as gas. C atoms left behind on the Cu surface start to form in-plane σ bonds (i.e., covalent bonds where each C atom relates to three other C atoms) and cover the whole Cu sheet continuously in a single layer [37]. If the growth time is long enough, a second or even a third layer may form. In this situation, van der Waals force of attraction is responsible to hold the layers together. Usually, a large number of C atoms, more than what is needed to form a single layer, gather near the grain boundaries; therefore, the quality of the graphene reduces in these areas [38].

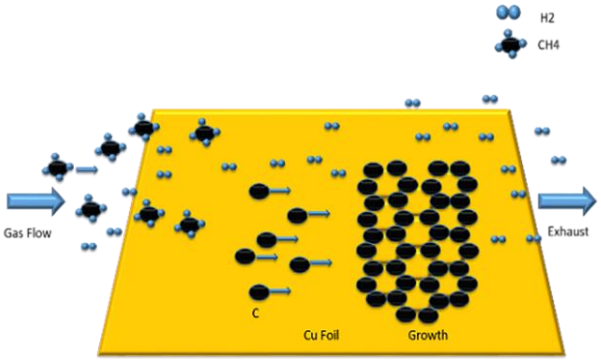

Figure 2. Schematics of LPCVD graphene growth mechanism on a Cu sheet

According to the FESEM images of the grown graphene samples shown in Figure 3 (top row), dark regions correspond to higher number of layers while bright regions correspond to lower number of layers. At higher growth temperatures, Cu surface becomes smoother in the lower number of grain boundaries. Higher temperatures are close to the melting point of Cu, thus providing much better growth conditions. At lower temperatures, higher surface roughness and larger number of grain boundaries would result in more nucleation and slow down the growth procedure [39]. According to the FESEM images, graphene domains are not continuous, hence more time is required to gain a continuous region of graphene. Of note, the number of graphene layers increases over time. In addition, increasing the growth time diminishes the growth process and creates anisotropic layers. These layers damage the existing layers. Here, the hydrogen flow, pressure, and evacuation rate (L/h) were adequate. Hydrogen controls the shape and size of the domains by breaking the hydrocarbon bonds. The pressure mainly affects the durability time of carbon atoms on the Cu surface. One of the reasons we worked at lower pressures was to prevent the saturation of carbon atoms and their nucleation on the Cu surface. By controlling these conditions, monolayer graphene with continuous layers can be achieved [40]. Optical images in Figure 3 (bottom row) show larger carbon crystallites in S1 with respect to S2 and S3. The grain boundaries in S2 and S3 are much more evident than in S1.

Raman spectra were taken from four random points on the graphene grown on the Cu sheets. Figure 4 shows the average the mentioned spectra for samples S1-S3. The Raman spectrum of the perfect single-layer graphene includes sp^2 hybridization with two peaks at 1580 cm^{-1} and 2700 cm^{-1} that are attributed to G and 2D bands, respectively [41].

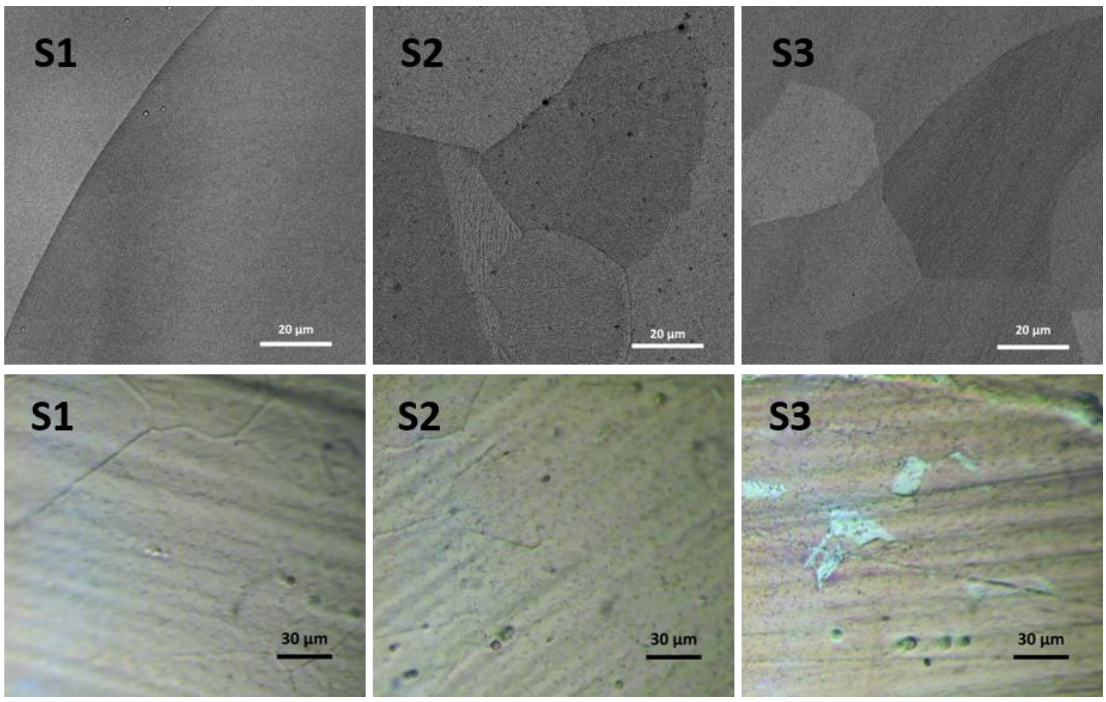

Figure 3. (Top row) FESEM images and (bottom row) optical images of S1-930 °C, S2-870 °C, and S3-760 °C, respectively

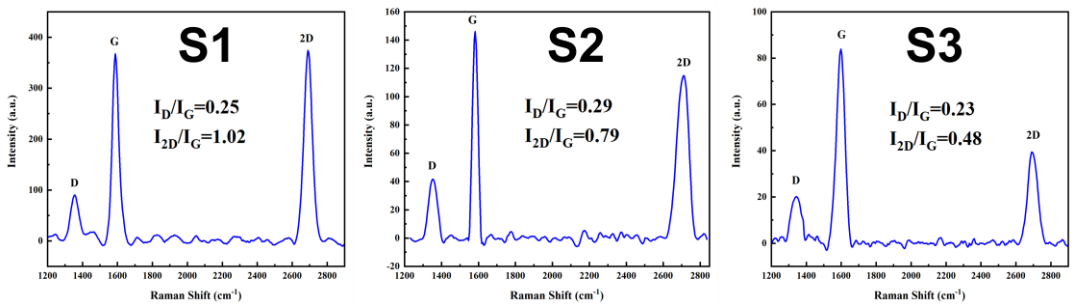

Figure 4. (Top row) FESEM images and (bottom row) optical images of S1-930 °C, S2-870 °C, and S3-760 °C, respectively

D band is observed when sufficient number of structural defects are reached for the graphene that leads to the intensification of the D band [42]. The ratio of I_{2D}/I_G=1.02, in sample S1 is larger than those of other samples due to its higher growth temperature which in turn leads to faster breaking of the bonds between H and C atoms and smoothing of the roughness on the substrate surface [32]. A comparison of the FESEM images of S1 with those of other samples shows that S1 consists of fewer layers. According to the averaged Raman spectrum analysis of S2, I_{2D}/I_G=0.79, which is less than that of S1. This result is consistent with the thickness and number of grain boundaries of the two samples shown in the FESEM images. According to the Raman spectrum of S3, I_{2D}/I_G = 0.48 which is lower than that of other samples. FESEM image of sample S3 showed more discontinuities and higher number of grain boundaries. The results obtained here are consistent with those acquired in previous studies [43]. Accordingly, at higher growth temperatures, I_{2D}/I_G ratio will increase which is indicative of a larger area of monolayer graphene. At higher growth temperatures, lower activation energy is required to break C-H bonds, thus resulting in the reduction of substrate roughness and the reduction of substrate grain boundaries [44]. S. Shukrullah et al. [45] investigated the effect of temperature on the activation energy. The coatings created therein were treated by CVD. The properties of the obtained coatings showed that the activation energy is inversely related to growth temperature, calculated by the following equation, known as the Arrhenius relation:

$$K = Ae^{-\frac{E_a}{RT}} \quad (1)$$

where K is the growth rate coefficient, E_a the activation energy, A the Arrhenius constant, R the global gas constant, and T the process temperature.

One of the important and comprehensive methods for identifying the structure of graphene and its morphological characteristics is AFM. The continuity of the grown layer and presence of impurities and surface roughness were confirmed through AFM and relevant analyses [46].

Roughness characterization is a very important tool before and after graphene transfer on the desired substrate. Many large-area graphene sheets suffer high roughness values that undermine their applications in electronic devices or even the separation membrane techniques. Therefore, controlling roughness via growth parameters is highly advantageous [47].

For a comparative study, the surface of the bare Cu sheet annealed at 930 °C was characterized in contact mode along with S1-S3 in tapping mode, all equipped with silicon nitride cantilevers. Figure 5 demonstrates a 3D view of the bare Cu and three graphene samples (S1-S3). As observed, the surface roughness in bare Cu, which was not exposed to methane, is higher than in the graphene-grown samples.

However, more quantitatively from roughness parameters extracted from topography images with SPIP software (Table 1), bare Cu is less rough than S3 probably due to the much lower annealing temperature Sample S3 went through than bare Cu did. Note that C crystallite structures on the surfaces of S1-S3 also increase the value of the roughness parameters while the bare Cu surface with no crystallites has relatively higher roughness values. In samples S1-S3, the average surface roughness or **Sa** increases from S1 to S3. **Sa**, is one of the most commonly used roughness parameters [48], and it is the average of the deviations of the mean plane. Another roughness parameter derived from the AFM topography images is **Sq** which is the standard deviation of the height distribution, also known as RMS roughness.

TABLE 1. Roughness parameters of bare Cu and graphene covered S1-S3, data extracted from AFM topographic images

parameters	Bare Cu	S1	S2	S3	Unit
Sa	20.4	6.9	16.9	21.3	nm
Sq	26.0	9.9	21.5	31.3	nm

Changes in this quantity are similar to changes in **Sa** in S1-S3. It is clear that increasing the growth temperature contributes to reduction in the deep structural roughness in the Cu sheet. Figure 6 shows 2D topographic and phase images of the samples. No trace of graphene is detected in the topographic or phase images of the bare Cu sample. According to the topographic images of samples S1-S3, some elements are observed on these surfaces, confirming the presence of a material different from the Cu sheet. Further, the surface structure in S1-S3 is significantly changed compared to that in the bare Cu which can be confirmed in the relevant phase images. In addition to the graphene grains, thicker carbon hexagonal structures can be seen on these surfaces, which is consistent with the findings of FESEM.

In addition, the number of impurities on these surfaces and thickness of the carbon crystallites (as bright spots) are in good agreement with the Raman spectroscopic findings for each sample. According to the phase images, the formation of grain boundaries in the grown graphene layers is evident. In S3, carbon crystallites as islands of thicker graphene (consisting of more layers) are obviously seen.

Figure 6 indicates the surface morphology of the samples, and Figure 4 shows the ratio of $I_{2D}/I_{G,}$ indicating the higher graphene coverage and more uniformity in samples S1-S3 followed by increasing growth temperature. This result is in agreement with the AFM results. In addition, based on the results from the topographic AFM images and Table 1, it can be concluded that the surface roughness decreases with an increase in the temperature. According to these results, there is a direct impact on the growth quality of graphene

mainly due to the sufficient energy provided to break the bond between hydrogen and carbon. At higher temperatures, this energy is given more to the carbon source gas that improves the growth coating quality and uniformity. In reality, several problems may arise such as limitation of the use of materials with lower melting points and high cost of experiments at high temperatures. Given these problems, another mechanism should be taken into account to produce the energy needed for breaking the bond between hydrogen and carbon. Consequently, high temperatures are not required for CVD graphene. This can be considered as the future research focus in this field.

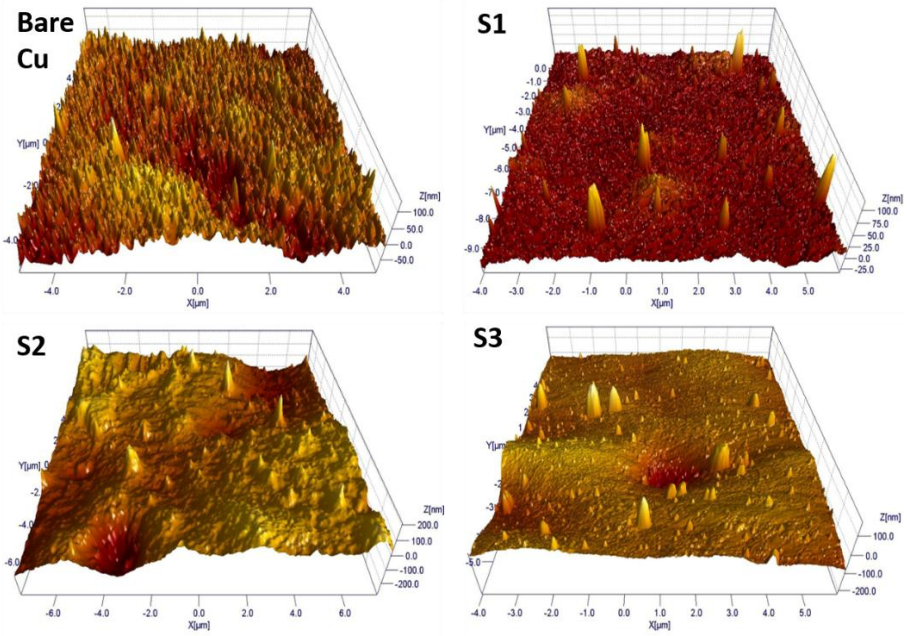

Figure 5. 3D images of the bare Cu and graphene grown in S1-S3. The size of all images is 10×10 μm^2

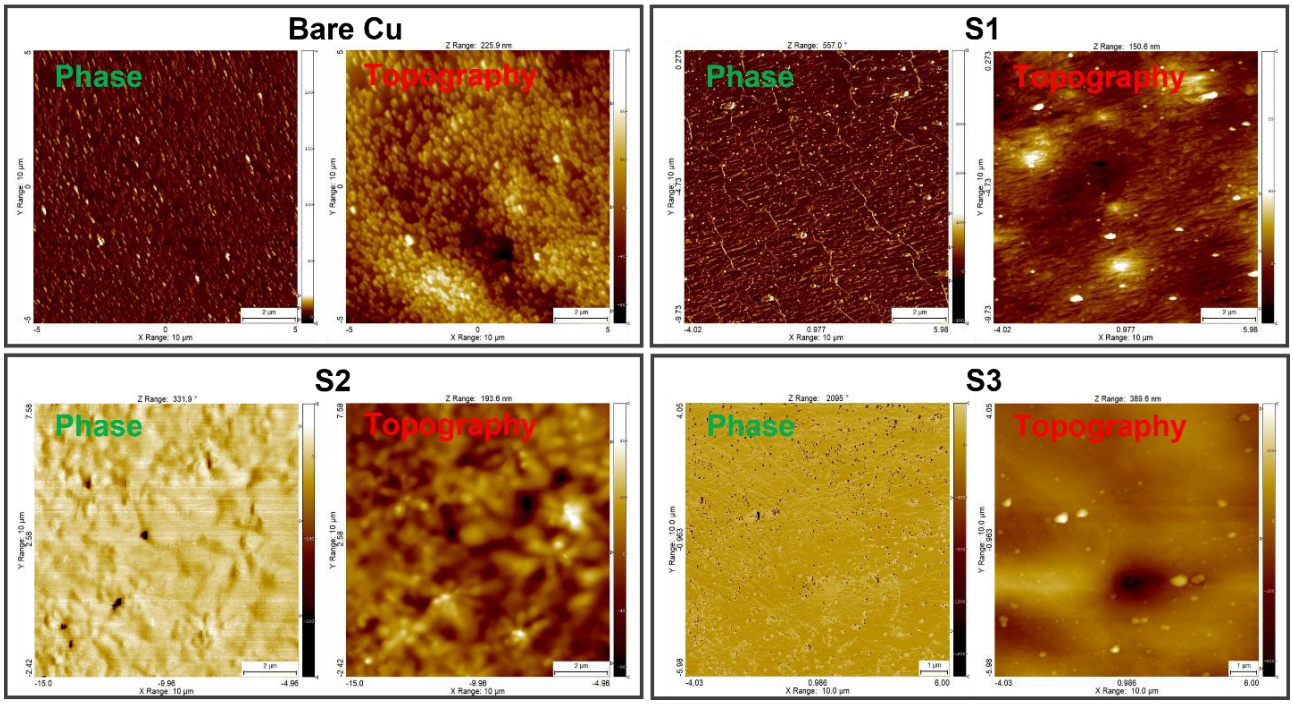

Figure 6. 2D topographic and the corresponding phase images of bare Cu and graphene covered S1-S3. All images are 10×10 μm^2

4. CONCLUSION

In this study, graphene was synthesized based on the LPCVD method using methane and hydrogen gas compounds on Cu catalysts at temperatures below 1000 °C. To this end, the conditions were optimized by keeping other growth parameters constant. According to the optical and FESEM analyses, the sample grown at 930 °C were characterized by better continuity and larger surface area than other samples. Based on the Raman spectroscopy analyses, it can be concluded that the ratio of I_{2D}/I_G at higher temperatures was higher than that at lower temperatures which, in this case, was indicative of the lower number of layers. The surface roughness from the AFM topographic images of the sample grown at 930 °C (6.935 nm) was less than that of the other two samples at 870 °C (16.953 nm) and 760 °C (21.328 nm). The measured roughness of the bare Cu (20.485 nm) was higher than S1 and S2 samples yet slightly lower than S3 sample. The obtained results confirmed the higher possibility of obtaining smoother graphene with better quality at higher temperatures.

ACKNOWLEDGEMENTS

The authors would like to thank National Elites Foundation No. 15/10002 in Iran for the financial support they provided towards this work.

REFERENCES

1. Wang, X., Song, Z., Wen, W., Liu, H., Wu, J., Dang, C., Hossain, M., Iqbal, M. A., Xie, L., "Potential 2D materials with phase transitions: structure, synthesis, and device applications", ***Advanced Materials***, Vol. 31, No. 45, (2019), 1804682. https://doi.org/10.1002/adma.201804682
2. Saraei, A., Eshraghi, M., Massoudi, A., "Investigation of resistive switching in anodized titanium dioxide thin films", ***Advanced Ceramics Progress***, Vol. 2, No. 3, (2016), 34-37. https://doi.org/10.30501/acp.2016.70029
3. Trivedi, S., Lobo, K., Matte, H. R., "Synthesis, properties, and applications of graphene", ***Fundamentals and Sensing Applications of 2D Materials***, (2019), 25-90. https://doi.org/10.1016/B978-0-08-102577-2.00003-8
4. Shi, G., Araby, S., Gibson, C. T., Meng, Q., Zhu, S., Ma, J., "Graphene platelets and their polymer composites: fabrication, structure, properties, and applications", ***Advanced Functional Materials***, Vol. 28, No. 19, (2018), 1706705. https://doi.org/10.1002/adfm.201706705
5. Malekpour, H., Chang, K. H., Chen, J. C., Lu, C. Y., Nika, D. L., Novoselov, K. S., Balandin, A. A., "Thermal conductivity of graphene laminate", ***Nano Letters***, Vol. 14, No. 9, (2014), 5155-5161. https://doi.org/10.1021/nl501996v
6. Li, W., Gao, S., Wu, L., Qiu, S., Guo, Y., Geng, X., Chen, M., Liao, S., Zhu, C., Gong, Y., Long, M., Xu, J., Wei, X., Sun, M., Liu, L., "High-density three-dimension graphene macroscopic objects for high-capacity removal of heavy metal ions", ***Scientific Reports***, Vol. 3, No. 1, (2013), 1-6. https://doi.org/10.1038/srep02125
7. Mak, K. F., Sfeir, M. Y., Wu, Y., Lui, C. H., Misewich, J. A., Heinz, T. F., "Measurement of the optical conductivity of graphene", ***Physical Review Letters***, Vol. 101, No. 19, (2008), 196405. https://doi.org/10.1103/PhysRevLett.101.196405
8. Papageorgiou, D. G., Kinloch, I. A., Young, R. J., "Mechanical properties of graphene and graphene-based nanocomposites", ***Progress in Materials Science***, Vol. 90, (2017), 75-127. https://doi.org/10.1016/j.pmatsci.2017.07.004
9. Samiee, M., Seyedraoufi, Z. S., Shajari, Y., "Dry and wet wear characteristic of TiO_2 thin film prepared by magnetic sputtering in ringer solution", ***Advanced Ceramics Progress***, Vol. 5, No. 4, (2019), 30-37. https://doi.org/10.30501/acp.2019.103893
10. Qiu, Y., Zhang, Y., Ademiloye, A. S., Wu, Z., "Molecular dynamics simulations of single-layer and rotated double-layer graphene sheets under a high velocity impact by fullerene", ***Computational Materials Science***, Vol. 182, (2020), 109798. https://doi.org/10.1016/j.commatsci.2020.109798
11. Yi, M., Shen, Z., "A review on mechanical exfoliation for the scalable production of graphene", ***Journal of Materials Chemistry A***, Vol. 3, No. 22, (2015), 11700-11715. https://doi.org/10.1039/C5TA00252D
12. Yu, P., Lowe, S. E., Simon, G. P., Zhong, Y. L., "Electrochemical exfoliation of graphite and production of functional graphene", ***Current Opinion in Colloid & Interface Science***, Vol. 20, No. 5-6, (2015), 329-338. https://doi.org/10.1016/j.cocis.2015.10.007
13. Xu, Y., Cao, H., Xue, Y., Li, B., Cai, W., "Liquid-phase exfoliation of graphene: an overview on exfoliation media, techniques, and challenges", ***Nanomaterials***, Vol. 8, No. 11, (2018), 942. https://doi.org/10.3390/nano8110942
14. Yazdi, G. R., Iakimov, T., Yakimova, R., "Epitaxial graphene on SiC: a review of growth and characterization", ***Crystals***, Vol. 6, No. 5, (2016), 53. https://doi.org/10.3390/cryst6050053
15. Kumar, A., Sharma, K., Dixit, A. R., "Carbon nanotube-and graphene-reinforced multiphase polymeric composites: review on their properties and applications", ***Journal of Materials Science***, Vol. 55, No. 7, (2020), 2682-2724. https://doi.org/10.1007/s10853-019-04196-y
16. Guex, L. G., Sacchi, B., Peuvot, K. F., Andersson, R. L., Pourrahimi, A. M., Ström, V., Farris, S., Olsson, R. T., "Experimental review: chemical reduction of graphene oxide (GO) to reduced graphene oxide (rGO) by aqueous chemistry", ***Nanoscale***, Vol. 9, No. 27, (2017), 9562-9571. https://doi.org/10.1039/C7NR02943H
17. Muñoz, R., Gómez-Aleixandre, C., "Review of CVD synthesis of graphene", ***Chemical Vapor Deposition***, Vol. 19, No. 10-11-12, (2013), 297-322. https://doi.org/10.1002/cvde.201300051
18. Bhuyan, M., Alam, S., Uddin, M., Islam, M., Bipasha, F. A., Hossain, S. S., "Synthesis of graphene", ***International Nano Letters***, Vol. 6, No. 2, (2016), 65-83. https://doi.org/10.1007/s40089-015-0176-1
19. Yang, X., Zhang, G., Prakash, J., Chen, Z., Gauthier, M., Sun, S., "Chemical vapour deposition of graphene: Layer control, the transfer process, characterisation, and related applications", ***International Reviews in Physical Chemistry***, Vol. 38, No. 2, (2019), 149-199. https://doi.org/10.1080/0144235X.2019.1634319
20. Venkatesan, S., Visvalingam, B., Mannathusamy, G., Viswanathan, V., Rao, A. G., "Effect of chemical vapor deposition parameters on the diameter of multi-walled carbon nanotubes", ***International Nano Letters***, Vol. 8, No. 4, (2018), 297-308. https://doi.org/10.1007/s40089-018-0252-4
21. Fallahazad, P., Naderi, N., Eshraghi, M. J., Massoudi, A., "Optimization of Chemical Texturing of Silicon Wafers Using Different Concentrations of Sodium Hydroxide in Etching Solution", ***Advanced Ceramics Progress***, Vol. 3, No. 3, (2017), 16-18. https://doi.org/10.30501/acp.2017.90753
22. Coraux, J., N 'Diaye, A. T., Busse, C., Michely, T., "Structural coherency of graphene on Ir (111)", ***Nano Letters***, Vol. 8, No. 2,

(2008), 565-570. https://doi.org/10.1021/nl0728874

23. Karu, A. E., Beer, M., "Pyrolytic formation of highly crystalline graphite films", ***Journal of Applied Physics***, Vol. 37, No. 5, (1966), 2179-2181. https://doi.org/10.1063/1.1708759
24. Land, T.A., Michely, T., Behm, R. J., Hemminger, J. C., Comsa, G., "STM investigation of single layer graphite structures produced on Pt (111) by hydrocarbon decomposition", ***Surface science***, Vol. 264, No. 3, (1992), 261-270. https://doi.org/10.1016/0039-6028(92)90183-7
25. Ullah, Z., Riaz, S., Li, Q., Atiq, S., Saleem, M., Azhar, M., Naseem, S., Liu, L., "A comparative study of graphene growth by APCVD, LPCVD and PECVD", ***Materials Research Express***, Vol. 5, No. 3, (2018), 035606. https://doi.org/10.1088/2053-1591/aab7b4
26. Ferrari, A. C., Bonaccorso, F., Fal'Ko, V., Novoselov, K. S., Roche, S., Bøggild, P., Borini, S., Koppens, F. H., Palermo, V., Pugno, N., Garrido, J. A., "Science and technology roadmap for graphene, related two-dimensional crystals, and hybrid systems", ***Nanoscale***, Vol. 7, No. 11, (2015), 4598-4810. https://doi.org/10.1039/C4NR01600A
27. Hamidi, S., Rahimipour, M. R., Eshraghi, M. J., Esfahani, H., "Optimization of Heat Treatment Cycles in Sub-atmospheric LiF-NaF-KF Based Fluoride Ion Cleaning for Removing Oxide Layers in Cracks of IN738-LC", ***Advanced Ceramics Progress***, Vol. 7, No. 1, (2021), 18-24. https://doi.org/10.30501/acp.2021.251522.1046
28. Taira, T., Obata, S., Saiki, K., "Nucleation site in CVD graphene growth investigated by radiation-mode optical microscopy", ***Applied Physics Express***, Vol. 10, No. 5, (2017), 055502. https://doi.org/10.7567/APEX.10.055502
29. Yao, Y., Li, Z., Lin, Z., Moon, K. S., Agar, J., Wong, C., "Controlled growth of multilayer, few-layer, and single-layer graphene on metal substrates", ***The Journal of Physical Chemistry C***, Vol. 115, No. 13, (2011), 5232-5238. https://doi.org/10.1021/jp109002p
30. Guermoune, A., Chari, T., Popescu, F., Sabri, S. S., Guillemette, J., Skulason, H. S., Szkopek, T., Siaj, M., "Chemical vapor deposition synthesis of graphene on copper with methanol, ethanol, and propanol precursors", ***Carbon***, Vol. 49, No. 13, (2011), 4204-4210. https://doi.org/10.1016/j.carbon.2011.05.054
31. Zhang, B., Lee, W. H., Piner, R., Kholmanov, I., Wu, Y., Li, H., Ji, H., Ruoff, R. S., "Low-temperature chemical vapor deposition growth of graphene from toluene on electropolished copper foils", ***ACS Nano***, Vol. 6, No. 3, (2012), 2471-2476. https://doi.org/10.1021/nn204827h
32. Chaitoglou, S., Bertran, E., "Effect of temperature on graphene grown by chemical vapor deposition", ***Journal of Materials Science***, Vol. 52, No. 13, (2017), 8348-8356. https://doi.org/10.1007/s10853-017-1054-1
33. Li, Z., Wu, P., Wang, C., Fan, X., Zhang, W., Zhai, X., Zeng, C., Li, Z., Yang, J., Hou, J., "Low-temperature growth of graphene by chemical vapor deposition using solid and liquid carbon sources", ***ACS Nano***, Vol. 5, No. 4, (2011), 3385-3390. https://doi.org/10.1021/nn200854p
34. Zheng, L., Cheng, X., Ye, P., Shen, L., Wang, Q., Zhang, D., Gu, Z., Zhou, W., Wu, D., Yu, Y., "Decreasing graphene synthesis temperature by catalytic metal engineering and thermal processing", ***RSC Advances***, Vol. 8, No. 3, (2018), 1477-1480. https://doi.org/10.1039/C7RA11654C
35. Mahyuddina, A., Ismaila, A. K., Firdaus, M., Omara, A. H. K., "Recent Progress on CVD Growth of Graphene from a Liquid Carbon Precursor", ***Malaysian Journal of Fundamental and Applied Sciences***, Vol. 17, No. 3, (2021), 262-273. https://doi.org/10.11113/mjfas.v17n3.2080
36. Huang, M., Ruoff, R. S., "Growth of single-layer and multilayer graphene on Cu/Ni alloy substrates", ***Accounts of Chemical Research***, Vol. 53, No. 4, (2020), 800-811. https://doi.org/10.1021/acs.accounts.9b00643
37. Seah, C. M., Chai, S. P., Mohamed, A. R., "Mechanisms of graphene growth by chemical vapour deposition on transition metals", ***Carbon***, Vol. 70, (2014), 1-21. https://doi.org/10.1016/j.carbon.2013.12.073
38. Vlassiouk, I., Smirnov, S., Regmi, M., Surwade, S. P., Srivastava, N., Feenstra, R., Eres, G., Parish, C., Lavrik, N., Datskos, P., Dai, S., "Graphene nucleation density on copper: fundamental role of background pressure", ***The Journal of Physical Chemistry C***, Vol. 117, No. 37, (2013), 18919-18926. https://doi.org/10.1021/jp4047648
39. Xing, S., Wu, W., Wang, Y., Bao, J., Pei, S. S., "Kinetic study of graphene growth: Temperature perspective on growth rate and film thickness by chemical vapor deposition", ***Chemical Physics Letters***, Vol. 580, (2013), 62-66. https://doi.org/10.1016/j.cplett.2013.06.047
40. Kim, H., Mattevi, C., Calvo, M. R., Oberg, J. C., Artiglia, L., Agnoli, S., Hirjibehedin, C. F., Chhowalla, M., Saiz, E., "Activation energy paths for graphene nucleation and growth on Cu", ***ACS Nano***, Vol. 6, No. 4, (2012), 3614-3623. https://doi.org/10.1021/nn3008965
41. Malard, L. M., Pimenta, M. A., Dresselhaus, G., Dresselhaus, M. S., "Raman spectroscopy in graphene", ***Physics Reports***, Vol. 473, No. 5-6, (2009), 51-87. https://doi.org/10.1016/j.physrep.2009.02.003
42. Thomsen, C., Reich, S., "Double resonant Raman scattering in graphite", ***Physical Review Letters***, Vol. 85, No. 24, (2000), 5214. https://doi.org/10.1103/PHYSREVLETT.85.5214
43. Wu, J. B., Lin, M. L., Cong, X., Liu, H. N., Tan, P. H., "Raman spectroscopy of graphene-based materials and its applications in related devices", ***Chemical Society Reviews***, Vol. 47, No. 5, (2018), 1822-1873. https://doi.org/10.1039/C6CS00915H
44. Zhang, Y. Y., Gu, Y., "Mechanical properties of graphene: Effects of layer number, temperature and isotope", ***Computational Materials Science***, Vol. 71, (2013), 197-200. https://doi.org/10.1016/j.commatsci.2013.01.032
45. Shukrullah, S., Mohamed, N. M., Shaharun, M. S., Saheed, M. S. M., Irshad, M. I., "Effect of CVD process temperature on activation energy and structural growth of MWCNTs", ***Metallurgical and Materials Transactions A***, Vol. 47, No. 3, (2016), 1413-1424. https://doi.org/10.1007/s11661-015-3303-8
46. Shen, Z., Li, J., Yi, M., Zhang, X., Ma, S., "Preparation of graphene by jet cavitation", ***Nanotechnology***, Vol. 22, No. 36, (2011), 365306. https://doi.org/10.1088/0957-4484/22/36/365306
47. Sharma, I., Dhakate, S. R., Subhedar, K. M., "CVD growth of continuous and spatially uniform single layer graphene across the grain boundary of preferred (111) oriented copper processed by sequential melting–resolidification–recrystallization", ***Materials Chemistry Frontiers***, Vol. 2, No. 6, (2018), 1137-1145. https://doi.org/10.1039/C8QM00082D
48. Yao, Y., Ren, L., Gao, S., Li, S., "Histogram method for reliable thickness measurements of graphene films using atomic force microscopy (AFM)", ***Journal of Materials Science & Technology***, Vol. 33, No. 8, (2017), 815-820. https://doi.org/10.1016/j.jmst.2016.07.020